DOI: 10.1002/ejic.200900763

Synthesis, X-ray Crystal Structures, DNA Binding and Nuclease Activities of Two Novel 1,2,4-Triazole-Based Cu^{II} Complexes

Dong-Dong Li,[a] Jin-Lei Tian,*[a] Wen Gu,[a] Xin Liu,[a] and Shi-Ping Yan*[a]

Keywords: DNA cleavage / DNA oxidation / Copper

Two novel 1,2,4-triazole-based copper(II) complexes have been synthesized and structurally characterized by X-ray crystallography: $[Cu_2LCl_3]\cdot 0.5[CuCl_4]\cdot EtOH$ (**1**) and $[Cu_2LBr_3]\cdot Br\cdot H_2O$ (**2**) (L = 3,5-bis{[bis(2-methoxyethyl)amino]-methyl}-4*H*-1,2,4-triazol-4-amine). Single-crystal diffraction reveals that the two Cu atoms have a distorted octahedral geometry for **2**, but one Cu atom is in a distorted square-pyramidal environment and the other one is in a distorted octahedral environment for **1** because of the different bridged halogen atoms. The interactions of the two complexes with calf thymus DNA (CT-DNA) have been investigated by UV absorption, fluorescence spectroscopy, circular dichroism spectroscopy, viscosity measurements and cyclic voltammetry. The apparent binding constant (K_{app}) values for complexes **1** and **2** are 2.98×10^6 and 4.05×10^6 M^{-1}. Furthermore, both the compounds display efficient oxidative cleavage of supercoiled DNA in the presence of external agents. The rate constants for the conversions of supercoiled to nicked DNA are 4.38×10^{-4} s^{-1} (for **1**) and 5.26×10^{-4} s^{-1} (for **2**).

Introduction

Artificial metallonucleases have been given much attention because of their diverse application in gene regulation, mapping of protein and DNA interactions, probing of DNA specific structures, and in cancer therapy.[1–4] Natural nucleases cleave the phosphate diester backbone of DNA by hydrolysis,[5] but the phosphodiester linkages of DNA are very stable to hydrolysis; their half-life for spontaneous hydrolysis is estimated to be 10^{11} years at pH 7 at 25 °C.[6] Chemical nucleases could cleave DNA by oxidative, photo-induced and hydrolytic processes;[7–12] they present some advantages over conventional enzymatic nucleases in that they are smaller and thus can reach more sterically hindered regions of a macromolecule. Many of them utilize the redox properties of the metal and dioxygen to produce reactive oxygen species that oxidize DNA, yielding direct strand scission or base modification.[13] Transition-metal complexes have been reported to mediate DNA oxidation in the presence of oxidants or reductants or without any assistant agents.[8,9,14–18] The typical Fenton-type reaction produces hydroxyl radicals that are responsible for the nonselective DNA scission induced by $[Fe(EDTA)]^{2-}$.[19] $[Cu(phen)_2]^{2+}$ induces direct strand damage in the presence of H_2O_2,[20] in which Cu^{II} species are required by a nondiffusible intermediate equivalent to hydroxyl radical to cleave one strand of the duplex. Fe-BLMs can promote DNA cleavage through the reaction of Fe^{III}–OOH or Fe^{IV}–O with C′4–H in the minor groove.[21]

There are several compounds involving a 1,2,4-triazole moiety having a wide range of biological and pharmacological activities such as antibacterial, antiviral, antiproliferative, antitumoral, fungicidal, herbicidal and analgesic.[22–24] For example, Marchiò et al. have reported two copper compounds of *cis*-[CuCl(HL)]Cl {HL = 1,4-dihydro-4-amino-3-(2-pyridyl)-5-thioxo-1,2,4-triazole} and *cis*-[CuCl(L^1)] {L^1 = 4-amino-5-methylthio-3-(2-pyridyl)-1,2,4-triazole} exerting significant antiproliferative activity of both normal and neoplastic cells.[24] Three Cu^{II} complexes of 5-amino-3-pyridin-2-yl-1,2,4-triazole (Hapt) showed high nuclease activity with ascorbate and H_2O_2 activation; Ferrer suggests that the reactive oxygen species involved in the DNA strand scission are hydroxyl·OH and probably $^1O_2$.[5] But investigation of the nuclease activity of halo-bridged 1,2,4-triazole-based complexes has not been reported recently, so we have begun to explore it. Here, we have synthesized two novel chloro-bridged and bromo-bridged 1,2,4-triazole-based Cu^{II} complexes, and reported the X-ray structures, DNA binding and nuclease activity. The results show that the two complexes can efficiently cleave DNA in the presence of external agents.

Results and Discussion

X-ray Structure Characterization

Complexes **1** and **2** have been structurally characterized by X-ray crystallography (Figure 1). Complex **1** consists of

[a] Department of Chemistry, Nankai University, Tianjin 300071, P. R. China
Fax: +86-022-23502779
E-mail: yansp@nankai.edu.cn
Supporting information for this article is available on the WWW under http://dx.doi.org/10.1002/ejic.200900763.

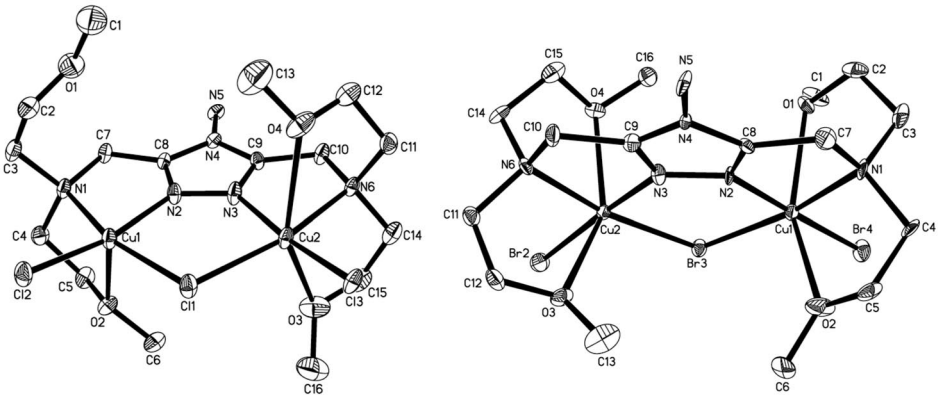

1 **2**

Figure 1. ORTEP view of $[Cu_2LCl_3]^+$ cation in **1** and $[Cu_2LBr_3]^+$ cation in **2**. Thermal ellipsoids are drawn at the 30% probability level.

one $[Cu_2LCl_3]^+$ cation, half a $[CuCl_4]^{2-}$ anion and one noncoordinated ethanol molecule. Cu(1) and Cu(2) atoms have different coordinated geometry. The Cu(1) atom is in a distorted square-pyramidal arrangement and this is reflected in the index of trigonality τ (0.05). (τ = 0 for a perfect square-pyramidal and 1 for a perfect trigonal-bipyramidal coordination sphere according to the Addison/Reedijk geometric criterion.)[25] N(1), N(2), Cl(1) and Cl(2) make up the equatorial plane and O(2) occupies the apical position. The apical bond length Cu(1)–O(2) is 2.278 Å. Cu(1) did not bond with O(1) because of the large distance of 3.844 Å between the Cu(1) and O(1). Cu(2) is in a distorted octahedral environment with N(3), N(6), Cl(3) and Cl(1) making up the equatorial plane and O(3) and O(4) occupying the apical position. The apical bond lengths Cu(2)–O(3) and Cu(2)–O(4) are 2.337 and 2.574 Å, and the angle O(3)–Cu(2)–O(4) is 149.98°. The typical Jahn–Teller effects influence Cu(2) in an elongated octahedral environment. The two chloro-bridged Cu atoms have a Cu(1)–Cl(1)–Cu(2) angle of 107.46° and the distance of Cu(1)···Cu(2) is 3.835 Å. The bridging bonds Cu(1)–Cl(1) = 2.367 Å and Cu(2)–Cl(1) = 2.390 Å are larger than the terminal Cu–Cl bonds [Cu(1)–Cl(2) = 2.183 Å, Cu(2)–Cl(3) = 2.195 Å]. This is similar to the reported $[Cu_2(pz)(phen)_2Cl_3]\cdot 2H_2O$,[26] in which the Cu–Cl (bridged) bond (2.570 Å) is longer than the Cu–Cl (terminal) bond (2.480 Å).

Complex **2** consists of one $[Cu_2LBr_3]^+$ cation, one Br^- anion and one noncoordinated water molecule. Both Cu(1) and Cu(2) atoms have a six-coordinate geometry with one 1,2,4-triazole-N atom, one tertiary amino-N atom, two alkyl O atoms, one terminal Br atom and one μ-Br atom as coordinated atoms; the two copper atoms are in a distorted octahedral environment. The 1,2,4-triazole bridging mode is a relatively symmetric one and it is reflected in the Cu(1)–N(2)–N(3) and Cu(2)–N(3)–N(2) angles (129.43 and 131.22°, respectively). The typical Jahn–Teller effects influence Cu atoms in an elongated octahedral environment. For Cu(1), the apical bond lengths Cu(1)–O(1) and Cu(1)–O(2) are 2.401 and 2.371 Å, and the angle O(2)–Cu(1)–O(1) is 151.36°. For Cu(2), the apical bond lengths Cu(2)–O(3) and Cu(2)–O(4) are 2.623 and 2.400 Å, and the angle O(3)–Cu(2)–O(4) is 146.05°. The two bromo-bridged Cu atoms have a Cu(1)–Br(3)–Cu(2) bond angle of 104.34° and the distance of Cu(1)···Cu(2) is 3.899 Å. The bridging bonds Cu(1)–Br(3) and Cu(2)–Br(3) are 2.484 and 2.453 Å, which are longer than the terminal Cu–Br bonds [Cu(1)–Br(4) 2.351 Å, Cu(2)–Br(2) 2.328 Å]; this is similar to complex **1**. The Cu···Cu distance in **2** is slightly longer than that in **1** because of the increased size of the exogenous bridging atom.

UV/Vis Absorption and Fluorescence Spectroscopy Studies

DNA binding is the critical step for DNA cleavage in most cases. Therefore, the binding ability of the complexes to CT-DNA was studied by using UV/Vis absorption and fluorescence spectroscopy. Firstly, the potential binding ability of complexes **1** and **2** to CT-DNA was studied by UV spectroscopy. The typical titration curves for complexes **1** and **2** are shown in Figure 2. The absorption peaks at 203 and 243 nm for **1**, and 206 and 246 nm for **2** are attributed to intraligand π–π* transition, as increased CT-DNA concentration, hypochromism of 39.8%–69.6% and redshifts of 19 nm for complexes **1** and **2** are observed at the maximal peak, and hypochromism of 12.8%–15.5% and redshifts of 30 nm (for **1**) and 31 nm (for **2**) are observed at the secondary peak (Table S1). This suggests intercalation between the complexes and DNA, because intercalation would lead to hypochromism and bathochromism in UV absorption spectra because of the intercalative mode involving a strong stacking interaction between an aromatic chromophore and the base pairs of DNA.[27] The extent of the hypochromism is commonly consistent with the strength of intercalative interaction.[28]

No luminescence is observed for complexes **1** and **2** at room temperature in aqueous solution. To further clarify the interaction of the complexes with DNA, a competitive binding experiment was carried out. EB emits intense fluorescence at about 600 nm in the presence of DNA because

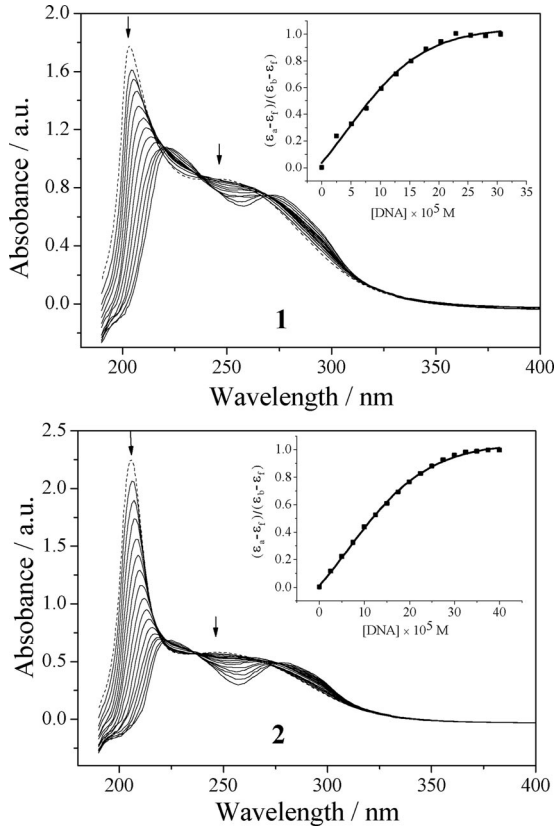

Figure 2. Absorption spectra of complexes **1** ([complex] = 1.96×10^{-4} M) and **2** ([complex] = 1.35×10^{-4} M) in the absence (dashed line) and presence (solid line) of increasing amounts of CT-DNA at room temperature in Tris-HCl/NaCl buffer (pH 7.2). Inset: plot of $(\varepsilon_a - \varepsilon_f)/(\varepsilon_b - \varepsilon_f)$ vs. [DNA] for absorption titration of CT-DNA with the complex.

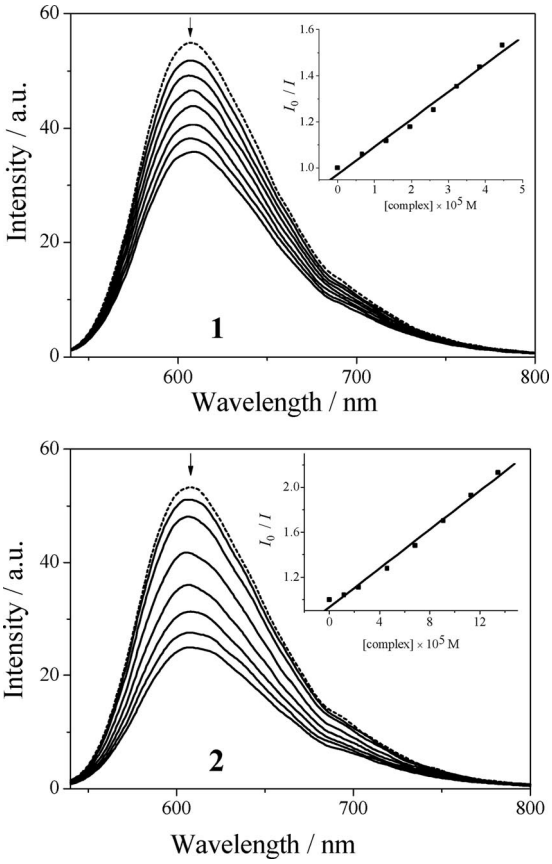

Figure 3. Fluorescence quenching curves of EB bound to DNA by complexes **1** ([complex] = 0–4.46×10^{-5} M) and **2** ([complex] = 0–1.35×10^{-4} M). The arrow shows the intensity changes on increasing the complex concentration. Inset: plot of I_0/I vs. [complex], λ_{ex} = 510 nm.

of its strong intercalation between the adjacent DNA base pairs.[29] It was previously reported that the enhanced fluorescence could be quenched by the addition of another molecule.[30] Two mechanisms have been proposed to account for this reduction in the emission intensity: the replacement of molecular fluorophores and/or electron transfer.[31] The relative binding of complexes **1** and **2** to CT-DNA was studied with an EB-bound CT-DNA solution in 5 mM Tris-HCl/50 mM NaCl buffer (pH 7.2) (Figure 3). Fluorescence intensities at 602 nm (510 nm excitation) were measured at different complex concentrations. The extent of reduction of the emission intensity gives a measure of the binding propensity of the complex to DNA. According to the classical Stern–Volmer equation,[32] the relative binding propensity of the complexes to CT-DNA was determined from the slope of straight line obtained from the plot of the fluorescence intensity versus the complex concentration. According to the equation K_{EB} [EB] = K_{app} [complex], where the complex concentration was the value at a 50% reduction of the fluorescence intensity of EB and K_{EB} = 1.0×10^7 M^{-1}, ([EB] = 50 μM). The apparent binding constants (K_{app}) at room temperature were calculated to be 2.98×10^6 M^{-1} for **1** and 4.05×10^6 M^{-1} for **2**, less than the binding constant of the classical intercalators and metallointercalators (10^7 M^{-1}).[33]

Circular Dichroism Study

The CD spectrum in the UV range is sensitive to the conformation changes of the helix and provides detailed information about the binding of the complex with DNA. The CD spectrum of CT-DNA exhibits a positive band at 275 nm because of base stacking and a negative band at 245 nm because of the helicity of B-type DNA.[34] While the groove binding interaction of small molecules with DNA shows few or no perturbations on the base stacking and helicity bands, intercalation enhances the intensities of both the bands, stabilizing the right-handed B conformation of CT-DNA. Figure 4 displays the CD spectra of CT-DNA in the absence or presence of complexes. When treated with complexes **1** and **2**, both the positive (ca. 275 nm) and negative (ca. 245 nm) bands decreased in intensity with redshift on addition of complexes, which is a clear indication of the interactions between the complexes and DNA. The decreased intensity in the negative band suggests the complex can unwind the DNA helix and lead to loss of helicity.[35] From the results of UV/Vis absorption, fluorescence and CD spectroscopic studies, we conclude that complexes **1** and **2** can effectively bind to CT-DNA.

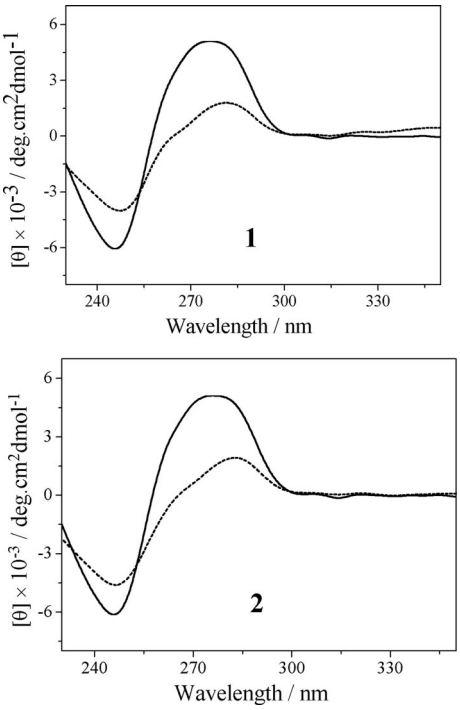

Figure 4. CD spectra of CT-DNA at 0.6 mM in the absence (solid line) and presence of 0.3 mM complexes **1** and **2** (dashed line).

Viscosity Measurements

As a means for further clarifying the binding of the complex, viscosity measurements were carried out on CT-DNA by varying the concentration of the complex. This is regarded as the most critical test of binding in solution in the absence of crystallographic structure data.[30] A significant increase in the viscosity of DNA on the addition of complex indicates the intercalative mode of binding to DNA. In contrast, complexes that bind in the DNA grooves by partial and/or nonclassical intercalation cause less pronounced (positive or negative) or no change in DNA solution viscosity.[36] Figure 5 shows the complexes cause a decrease in the relative viscosity of DNA. This may be explained by a binding mode that produced bends or kinks in the DNA and thus reduced its effective length and concomitantly its viscosity. The results suggest that the complexes may bind to DNA by partial intercalation.

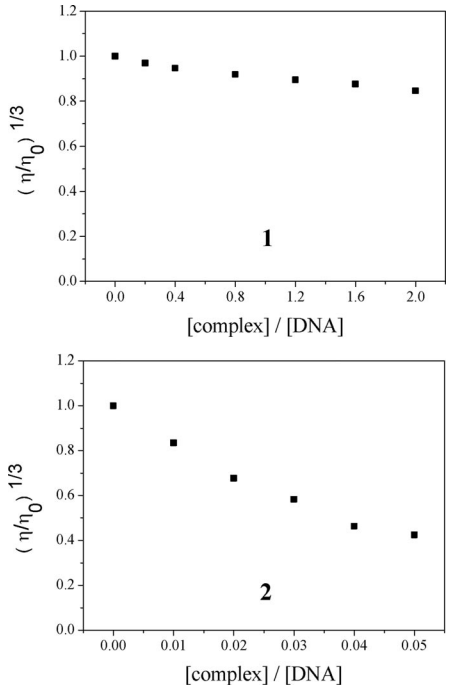

Figure 5. Effect of increasing amounts of the complexes on the relative viscosity of calf thymus DNA at (37 ± 0.1) °C in 5 mM Tris-HCl buffer (pH 7.2, [DNA] = 0.1 mM).

Electrochemical Study

The application of the cyclic voltammetric technique to the study of interactions between the metal complexes and DNA provides a useful complement to the previously used spectroscopic studies. Figure 6 shows the cyclic voltammograms of complexes **1** and **2** at different scan rates. Both complexes have been found to show two couples of waves corresponding to two one-electron redox processes of Cu^{II}-$Cu^{II}/Cu^{II}Cu^{I}$ and $Cu^{II}Cu^{I}/Cu^{I}Cu^{I}$. The ΔE_p increases with increasing scan rate (10, 50, 100, 150, 200 $mV s^{-1}$) and i_{pa}/i_{pc} values are not the same at different scan rates. The first reduction potentials are observed at E^1_{pc} = –0.021 and –0.007 V for complexes **1** and **2** at 100 $mV s^{-1}$; this can be assigned to the redox couple $Cu^{II}Cu^{II}/Cu^{II}Cu^{I}$. The second reduction potentials for complexes **1** and **2** are observed at E^2_{pc} = –0.578 and –0.543 V, which can be attributed to the redox couple $Cu^{II}Cu^{I}/Cu^{I}Cu^{I}$. Complex **2** reduced at less negative potentials than complex **1**, suggesting that the geometry around the copper ions in complex **2** is more distorted than the copper ions in complex **1**.

In the presence of CT-DNA, the cyclic voltammograms of the two copper(II) complexes exhibited shifts in the anodic and cathodic peak potentials followed by decreases in both peak currents, indicating an interaction between the two copper(II) complexes and CT-DNA. The drop of the voltammetric currents in the presence of CT-DNA can be attributed to diffusion of the metal complex bound to the large, slowly diffusing DNA molecule.[37] The $E_{1/2}$ values in the presence of CT-DNA exhibit negative shifts of 6 and 28 mV for **1**, and 3 and 31 mV for **2**; these detailed data can be seen in Table S2. The shift in the value of the formal potential ($\Delta E^{\circ\prime}$) can be used to estimate the ratio of equilibrium binding constants (K_R/K_O) according to the model of interaction described by Bard and Carter.[38] From this model one can obtain that:

$$\Delta E^{\circ\prime} = E_b^{\circ\prime} - E_f^{\circ\prime} = 59.15 \log(K_R/K_O)$$

where $E_b^{\circ\prime}$ and $E_f^{\circ\prime}$ are the formal potentials of the bound and free complex forms, and K_R and K_O are the corresponding binding constants for the binding of reduction and oxidation species to CT-DNA, respectively. The $K_{Cu}{}^{I}/K_{Cu}{}^{II}$ values are 1.26 and 2.97 for complex **1**, and 1.12 and

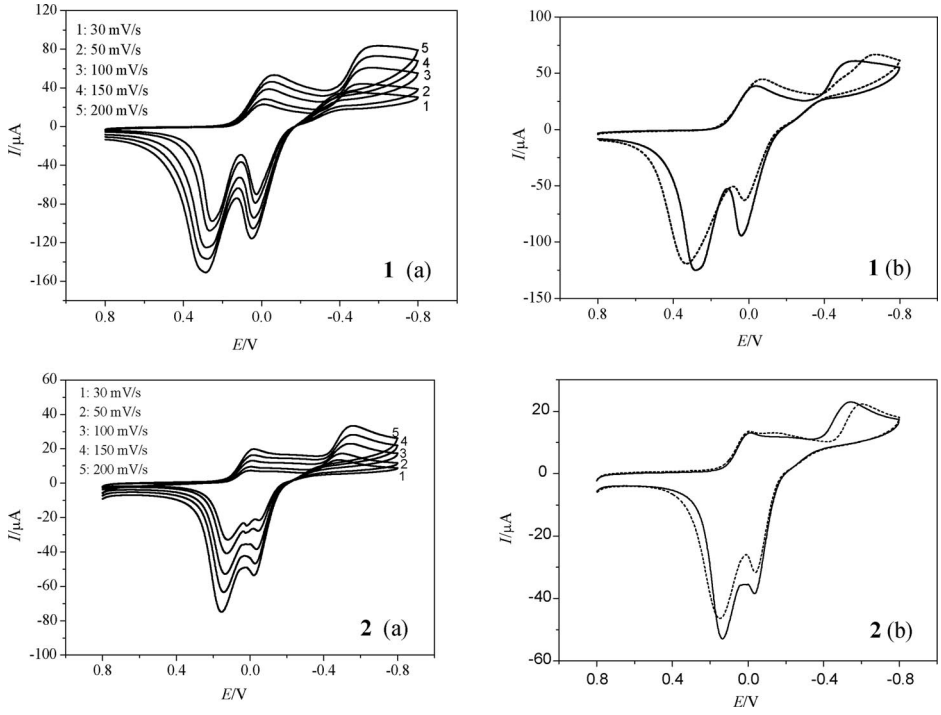

Figure 6. Cyclic voltammograms of complexes **1** and **2** at different scan rates, **1** (a) and **2** (a), and in the absence (solid line) and presence (dashed line) of CT-DNA in 10 mM Tris-HCl/50 mM NaCl buffer (pH 7.2), **1** (b) and **2** (b); scan rate: 100 mV s^{-1}.

3.34 for complex **2**, suggesting a stronger binding affinity in the Cu^{I} state than in the Cu^{II} state for both of the copper(II) complexes.

The values of the half-wave potential of the two redox processes and K_{con} are measures of the relative stability of the mixed valent $Cu^{II}Cu^{I}$ species. The $E_{1/2}$ value cannot be applied to asymmetrical complexes with two copper ions in different coordination environments. However the K_{con} value still characterizes the stability of mixed valent species.[39] According to the cyclic voltammograms of complexes **1** and **2**, the two reduction processes are assigned generally as follows,

$$M^{II}M^{II} \rightleftharpoons M^{II}M^{I} \rightleftharpoons M^{I}M^{I}$$

The stability of the mixed-valence $Cu^{I}Cu^{II}$ complexes is expressed by the conproportionaton constant K_{con} for the equilibrium:

$$M^{II}M^{II} + M^{II}M^{I} \overset{K_{con}}{\rightleftharpoons} 2M^{I}M^{I}$$

The values have been determined electrochemically using the equation $\log K_{con} = E_{1/2}/0.0591$ (at 25 °C), where $E_{1/2} = E^{1}_{1/2} - E^{2}_{1/2}$. The K_{con} values for the two complexes are calculated to be 6.85×10^{6} and 1.02×10^{6}, respectively.

The Cleavage of pBR322 DNA

The chemical nuclease activities of complexes **1** and **2** have been studied using supercoiled pBR322 plasmid DNA as a substrate in a medium of 50 mM Tris-HCl/NaCl buffer (pH 7.2) in the absence and presence of external agents under physiological conditions. When circular plasmid DNA is conducted by electrophoresis, the fastest migration will be observed for the supercoiled form (Form I). If one strand is cleaved, the supercoils will relax to produce a slower-moving nicked circular form (Form II). If both strands are cleaved, a linear form (Form III) will be generated which migrates in between Form I and Form II.

Firstly, the concentration-dependent DNA cleavage by complexes **1** and **2** was performed. A control experiment with copper(II) salt was also carried out under the same experimental conditions. Figure 7 shows the results of gel electrophoretic separations of plasmid pBR322 DNA induced by increasing concentration of the two complexes and copper salt in the absence of external agents at pH 7.2 (50 mM Tris-HCl/NaCl buffer) at 37 °C for 3 h. With the increase of the concentrations of the complexes, Form I

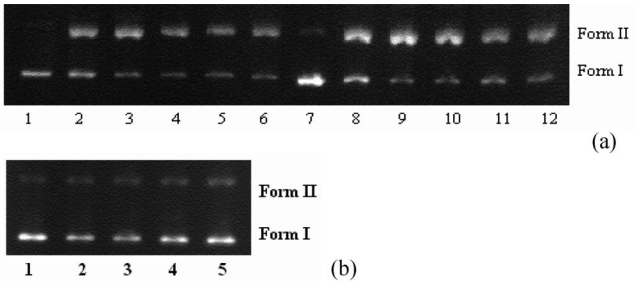

Figure 7. (a) Gel electrophoresis diagrams showing the cleavage of pBR322 DNA (0.1 μg μL^{-1}) at different complex concentrations in Tris-HCl/NaCl buffer (pH 7.2) and 37 °C. Lane 1: DNA control (3 h); lanes 2–6: DNA + **1** (0.18, 0.7, 1.2, 1.75, 2.8 mM); lane 7: DNA control (3 h); lanes 8–12: DNA + **2** (0.18, 0.7, 1.2, 1.75, 2.8 mM). (b) Lane 1: DNA control; lanes 2–5: DNA + **$CuCl_2$** (0.05, 0.2, 0.35, 0.5 mM, respectively).

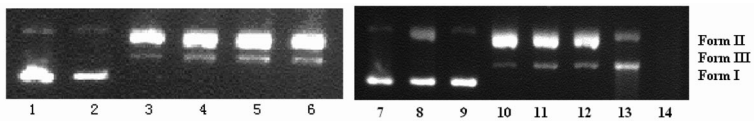

Figure 8. Gel electrophoresis diagrams showing the cleavage of pBR322 DNA (0.1 $\mu g \mu L^{-1}$) at different complex concentrations in Tris-HCl/NaCl buffer (pH 7.2) and 37 °C. Lane 1: DNA control (3 h); lane 2: DNA + 0.25 mM H_2O_2; lanes 3–6: DNA + 0.25 mM H_2O_2 + **1** (0.175, 0.875, 1.75, 2.625 mM); lane 7: DNA control (3 h); lane 8: DNA + 0.25 mM H_2O_2; lane 9: DNA + 0.0175 mM **2**; lanes 10–14: DNA + 0.25 mM H_2O_2 + **2** (0.0175, 0.0875, 0.175, 0.875, 1.75 mM).

plasmid DNA is gradually converted into Form II, but it is invisible for copper salt. The results indicate that the cationic complex plays a role in DNA cleavage for complex **1**.

In addition, we also investigated the cleavage activity of the two complexes in the presence of activators (here are H_2O_2, ascorbate and H_2O_2/ascorbate). Both complexes **1** and **2** were found to exhibit higher nuclease activity on treatment with the three different activators. As shown in Figure 8, both complexes **1** and **2** can convert supercoiled plasmid DNA to a mixture of nicked (Form II) and linear (Form III) DNA in the presence of H_2O_2, while at a concentration of 1.75 mM (lane 14, Figure 8) only smearing appears for **2**. This phenomenon could be seen in the reported documents.[5,40] Smearing was found for both complexes under the H_2O_2/ascorbate condition (lane 6 and 12, Figure 1S), whereas it could not be seen under the ascorbate condition (Figure 2S). The results indicate the following increasing order of efficiency: ascorbate < H_2O_2 < H_2O_2/ascorbate. Several authors have studied the influence of different activators on the cleavage of DNA by copper(II) complexes.[41–43] Sigman et al.[41] have found MPA to be superior to ascorbic acid as an activating agent on the nuclease activity of a bis(*o*-phenanthroline)–copper(II) complex because it produces less background cleavage. Chiou et al.[42] have shown that ascorbate is more effective in cleaving DNA than other reducing agents such as MPA and dithiothreitol because of its ability to generate hydrogen peroxide in the presence of oxygen and metal ions, whereas other reducing agents are known to produce superoxide, which rapidly undergoes dismutation in aqueous solution. Detmer et al.[43] have indicated a mixture of H_2O_2 and ascorbate is a more effective activating agent than ascorbate alone. In our study, we found that H_2O_2 and H_2O_2/ascorbate (1:1) are the best activators for DNA cleavage.

The time-dependent cleavage of DNA by complexes **1** and **2** was also studied. Figure 9 shows the results of gel electrophoretic separations of plasmid pBR322 DNA induced by increasing reaction time in the absence of external agent at pH 7.2 (50 mM Tris-HCl/NaCl buffer) at 37 °C. On increasing reaction time, Form I plasmid DNA is gradually converted into Form II. From Figure 10, we can find that all of them are typical pseudo-first-order consecutive reactions, which are consistent with the general model for enzyme-catalyzed reactions.[44,45] Fitting the experimental data with first-order consecutive kinetic equations, the rate constants of $4.38 \times 10^{-4}\ s^{-1}$ (for **1**) and $5.26 \times 10^{-4}\ s^{-1}$ (for **2**) for the conversions of supercoiled to nicked DNA are obtained.

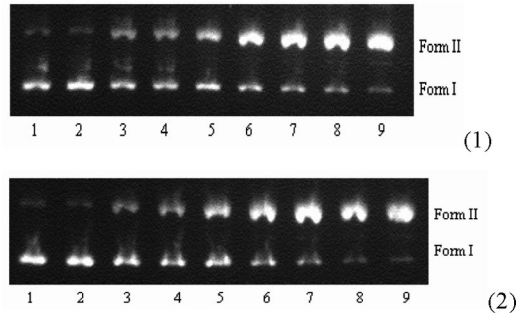

Figure 9. Time dependence of pBR322 DNA cleavage by 0.7 mM **1** and **2** in Tris-HCl/NaCl buffer (pH 7.2) at 37 °C. (1) Lane 1: DNA control (5 h); lanes 2–9: DNA + **1** (0, 0.17, 0.5, 1, 2, 3, 4, 5 h, respectively). (2) Lane 1: DNA control (5 h); lanes 2–9: DNA + **2** (0, 0.17, 0.5, 1, 2, 3, 4, 5 h, respectively).

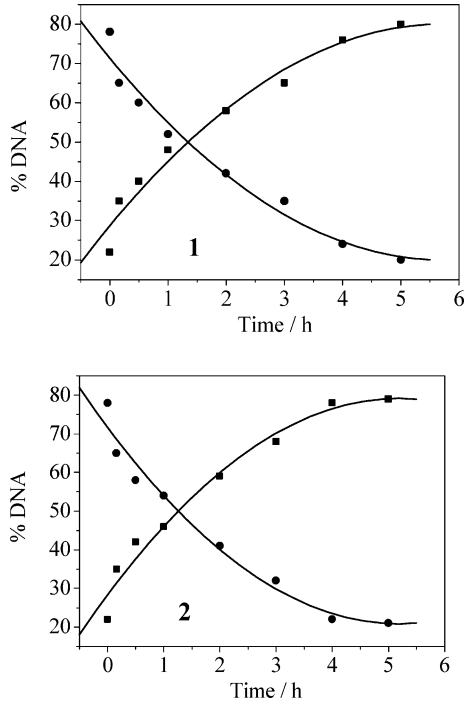

Figure 10. Disappearance of supercoiled (●) form and formation of nicked circular (■) form of plasmid DNA in the presence of complexes **1** and **2** with the incubation time.

DNA Cleavage Mechanism

Copper complexes can cleave DNA both through hydrolytic and oxidative processes. For the oxidative process, the complexes have been shown to react with molecular oxygen

or hydrogen peroxide to produce a variety of active oxidative intermediates (reactive oxygen species or nondiffusible copper–oxene species). In order to obtain information about the active chemical species that was responsible for the DNA damage, we investigated the DNA cleavage in the presence of hydroxyl radical scavengers (DMSO, EtOH), singlet oxygen quenchers (NaN_3, L-histidine), superoxide scavenger (SOD), hydrogen peroxide scavenger (KI) and chelating agent (EDTA)[46] under our experimental conditions. From Figure 11, we can see that no obvious inhibitions are observed for the two complexes in the presence of DMSO (lane 3), EtOH (lane 4) and SOD (lane 7). These results rule out the possibility of DNA cleavage by hydroxyl radical and superoxide. The EDTA, a Cu^{II}-specific chelating agent that strongly binds to Cu^{II}, forming a stable complex, can efficiently inhibit DNA cleavage, indicating Cu^{II} complexes play the key role in the cleavage. The addition of SYBR Green and methyl green, which are known to interact with DNA at minor and major grooves,[47,48] hardly inhibited DNA cleavage by complexes **1** and **2**. This result suggested that the complexes did not interact through grooves. NaN_3 (lane 5) and L-histidine (lane 6) significantly diminish the nuclease activity of the two compounds, which is indicative of the involvement of the singlet oxygen or a singlet oxygen-like entity in the cleavage process. This also can be seen from the inhibition of addition of potassium iodide. The inhibitory activity of sodium azide can be ascribed to the affinity of the azide anion for transition metals.[10] The copper(II) complexes examined here may be capable of promoting DNA cleavage through an oxidative DNA damage pathway. Probably a copper peroxide with DNA cleaving ability is formed by an active singlet oxygen species or a singlet oxygen-like entity. The assumed involvement of a copper-oxido species can be deduced from the reaction of copper(I) and endogenous dioxygen to give a superoxide anion that dismutates, giving rise to hydrogen peroxide that can react, yielding copper(I), to obtain a copper-oxido species. Sigman reports thiol potentiation of the 1,10-phenanthroline-copper [$(OP)_2Cu^{2+}$] complex, which cleaves DNA through generation of a copper-oxido species.[49,50] The higher nuclease efficiency of the two complexes in the presence of activators is probably due to the higher concentration of the Cu^{I} ions obtained.

The following is the proposed mechanistic pathway for the chemical nuclease activity of the two copper(II) complexes in the Tris-buffer medium. The first step is the interaction of the copper complex with DNA through the outer sphere while the second step consists of the reduction of the copper(II) complex to the copper(I) complex through reaction with the reducing agent. The copper(I) complex reacts with endogenous oxygen to obtain a superoxide anion and then the superoxide anion dismutates to produce hydrogen peroxide. Hydrogen peroxide reacts with another equivalent of Cu^{I} complex to produce a hydroxyl radical species that can bind to the metal ion. This species is considered analogous to a metal-oxido system and is responsible for the DNA damage. In this process, the hydroxyl radical was indeed produced in spite of the poor inhibition of the hydroxyl scavengers. There may be two reasons for this phenomenon. One is that the hydroxyl radical presents a high rate of decomposition (half-life 10^{-9} s),[51] which allows it to react with the deoxyribose portion of the DNA before the scavengers of hydroxyl radical can act. Another is that the produced hydroxyl radical is bound to the metal ion to form a metal–OOH peroxide complex, which could react with DNA, but is not trapped by hydroxyl scavengers.[52–54]

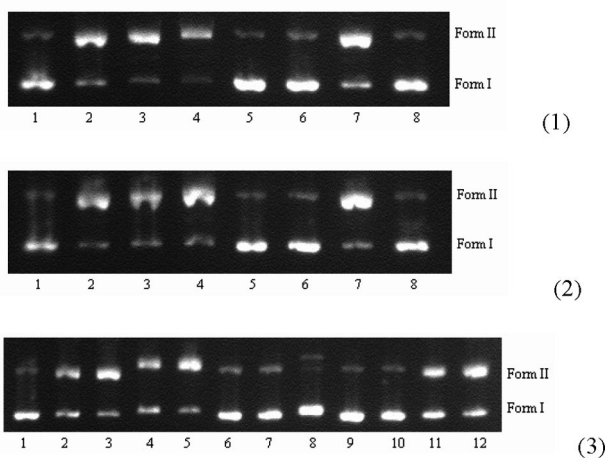

Figure 11. Agarose gel showing cleavage of pBR322 DNA (0.1 $\mu g\,\mu L^{-1}$) incubated with (1) **1** (0.7 mM) and (2) **2** (0.7 mM) in Tris-HCl/NaCl buffer (pH 7.2) at 37 °C for 3 h. Lane 1: DNA control; lane 2: DNA + complex; lane 3: DNA + complex + DMSO (5 μL); lane 4: DNA + complex + EtOH (5 μL); lane 5: DNA + complex + NaN_3 (50 mM); lane 6: DNA + complex + L-histidine (50 mM); lane 7: DNA + complex + SOD (10 $U\,mL^{-1}$); lane 8: DNA + complex + EDTA (250 mM). (3) Lane 1: DNA control; lane 2: DNA + **1** (0.35 mM); lane 3: DNA + **2** (0.35 mM); lane 4: DNA + **1** + SYBR Green (10 $U\,mL^{-1}$); lane 5: DNA + **2** + SYBR Green (10 $U\,mL^{-1}$); lane 6: DNA + **1** + KI (50 mM); lane 7: DNA + **2** + KI (50 mM); lane 8: DNA + SYBR Green (10 $U\,mL^{-1}$); lane 9: DNA + KI (50 mM); lane 10: DNA + methyl green (0.05 mM); lane 11: DNA + **1** + methyl green (0.05 mM); lane 12: DNA + **2** + methyl green (0.05 mM).

Cu^{II} complex + DNA → Cu^{II} complex···DNA

Cu^{II} complex + e^- → Cu^{I} complex

Cu^{I} complex + O_2 → Cu^{II} complex + O_2^-

O_2^- + $2H^+$ → H_2O_2 + O_2

Cu^{I} complex + H_2O_2 → copper-oxido species

copper-oxido species + DNA → DNA cleavage

Conclusions

In summary, although pyrazole-bridged complexes have been reported previously,[26,55–57] the study is concentrated on the structure and magnetism. Our work provides two halo-bridged 1,2,4-triazole-based Cu^{II} complexes showing efficient chemical nucleases in the presence of activators. The reactive oxygen species involved in the DNA strand scission are singlet oxygen or a singlet oxygen-like entity.

The strong DNA binding ability coupled with the potent DNA cleavage activity of complexes **1** and **2** shows potential for targeted DNA oxidative damage.

Experimental Section

Materials and Instrumentation: The ligand L was synthesized according to the literature procedure.[58] Ethidium bromide (EB), calf thymus DNA (CT-DNA) and pBR322 plasmid DNA were from Sigma. Tris-HCl buffer solution was prepared using deionized sonicated triple-distilled water. All other chemicals used were of analytical grade. Solution of the copper(II) complex and other reagents used for strand scission were prepared freshly in triple-distilled water before use. Solvents used in this research were purified by standard procedures.

Elemental analyses for C, H and N were obtained on a Perkin–Elmer analyser model 240. Infrared spectroscopy on KBr pellets was performed on a Bruker Vector 22 FTIR spectrophotometer in the 4000–400 cm^{-1} regions. The electronic spectra were measured on a JASCO V-570 spectrophotometer. The fluorescence spectroscopic data were obtained on a MPF-4 fluorescence spectrophotometer at room temperature. The Gel Imaging and documentation DigiDoc-It System were assessed using Labworks Imaging and Analysis Software (UVI, England). The circular dichroism (CD) spectra were taken on a JASCO-J715 spectropolarimeter.

$[Cu_2LCl_3]\cdot 0.5[CuCl_4]\cdot EtOH$ (1): An ethanolic solution (4 mL) of L (0.0004 mol) was added dropwise to an aqueous solution (10 mL) of $CuCl_2\cdot 2H_2O$ (0.0008 mol, 0.1364 g) and the resulting solution was refluxed for 4 h, cooled and filtered. Green block crystals suitable for X-ray diffraction were obtained by slow evaporation of the green filtrate, collected by filtration, washed with diethyl ether and dried in air. (Yield 37%, 0.086 g) $C_{16.75}H_{35.5}Cl_5Cu_{2.5}N_6O_{4.25}$ (725.11): calcd. C 27.74, H 4.94, N 11.59; found C 27.65, H 5.15, N 11.48. IR (KBr): $\tilde{\nu}$ = 3300, 2933, 1625, 1574, 1448, 1109, 1051, 1005, 859 cm^{-1}.

$[Cu_2LBr_3]\cdot Br\cdot H_2O$ (2): Complex **2** was prepared in a similar way to that of complex **1** except $CuBr_2$ (0.0008 mol, 0.1787 g) was used instead of $CuCl_2\cdot 2H_2O$ (0.0008 mol, 0.1364 g). Slow evaporation of the filtrate at room temperature provided brown block crystals suitable for X-ray diffraction. (Yield 39%, 0.13 g). $C_{16}H_{36}Br_4Cu_2N_6O_5$ (839.21): calcd. C 22.90, H 4.32, N 10.01; found C 22.81, H 4.45, N 9.95. IR (KBr): $\tilde{\nu}$ = 3282, 2938, 2898, 1624, 1568, 1447, 1110, 1048, 990, 866 cm^{-1}.

X-ray Crystallography: Suitable single crystals with approximate dimensions of $0.14\times0.08\times0.08$ mm (for **1**) and $0.12\times0.10\times0.08$ mm (for **2**) were used for X-ray diffraction analyses. Diffraction data for **1** and **2** were collected at 293(2) K with a Bruker Smart 1000 CCD diffractometer using Mo-K_α radiation (λ = 0.71073 Å) with the ω-2θ scan technique. The structure was solved by direct methods (SHELXS-97) and refined with the full-matrix least-squares technique on F^2 using SHELXL-97.[59,60] The hydrogen atoms were added theoretically, as riding atoms on the relevant atoms and refined with fixed thermal factors. Details of the crystallographic data and structure refinement parameters are summarized in Table 1. Selected bond angles and distances are listed in Table 2.

CCDC-713620 (for **1**) and -713621 (for **2**) contain the supplementary crystallographic data for this paper. These data can be obtained free of charge from The Cambridge Crystallographic Data Centre via www.ccdc.cam.ac.uk/data_request/cif.

Absorption Spectroscopic Studies: The UV absorbance at 260 nm and 280 nm of the CT-DNA solution in 5 mM Tris-HCl/50 mM NaCl buffer (pH 7.2) gives a ratio of 1.8–1.9, indicating that the DNA was sufficiently free of protein.[61] The concentration of CT-DNA was determined from its absorption intensity at 260 nm with a molar extinction coefficient of 6600 $M^{-1}cm^{-1}$.[62] The absorption

Table 1. Crystallographic data and structure refinement parameters for complexes **1** and **2**.

Complex	**1**	**2**
Empirical formula	$C_{16.75}H_{35.50}Cl_5Cu_{2.50}N_6O_{4.25}$	$C_{16}H_{36}Br_4Cu_2N_6O_5$
Formula weight	725.11	839.21
Temperature /K	293(2)	293(2)
Wavelength /Å	0.71073	0.71073
Crystal system, space group	monoclinic, *C*2/*c*	orthorhombic, *Pna*2(1)
a /Å	23.691(5)	21.657(4)
b /Å	14.565(3)	7.6898(15)
c /Å	20.389(4)	32.913(7)90
α /°	90	90
β /°	123.69(3)	90
γ /°	90	90
Volume /Å^3	5891(2)	5481.3(19)
Z, calculated density /mg m^{-3}	8, 1.635	8, 2.034
Absorption coefficient /mm^{-1}	2.283	7.421
F(000)	2956	3296
Crystal size /mm	$0.14\times0.08\times0.08$	$0.12\times0.10\times0.08$
Theta range for data collection /°	1.73–25.02	1.88–25.02
Limiting indices, *hkl*	–26 to 28, –14 to 17, 24 to 23	–25 to 25, –9 to 9, –39 to 35
Reflections collected/unique	17254/5194	30739/8502
R_{int}	0.1121	0.0877
Absorption correction	semiempirical	semiempirical
Max. and min. transmission	0.8384 and 0.7405	0.5882 and 0.4696
Data/restraints/parameters	5194/174/324	8562/19/604
Goodness-of-fit on F^2	1.026	1.029
Final *R* indices [$I > 2\sigma(I)$]	R_1 = 0.0634, wR_2 = 0.1504	R_1 = 0.0528, wR_2 = 0.1242
R indices (all data)	R_1 = 0.0845, wR_2 = 0.1650	R_1 = 0.0671, wR_2 = 0.1333
Largest difference peak and hole/e Å^{-3}	1.294 and –0.671	1.120 and –1.202

Table 2. Selected bond lengths [Å] and angles [°] for complexes **1** and **2**.

Complex **1**			
Cu(1)–N(2)	1.919(5)	Cu(1)–N(1)	2.161(5)
Cu(1)–Cl(2)	2.183(2)	Cu(1)–O(2)	2.278(4)
Cu(1)–Cl(1)	2.367(2)	Cu(2)–N(3)	1.929(5)
Cu(2)–N(6)	2.185(5)	Cu(2)–Cl(3)	2.195(2)
Cu(2)–O(3)	2.337(4)	Cu(2)–Cl(1)	2.390 (2)
Cu(1)···Cu(2)	3.835(2)	Cu(2)–O(4)	2.574(8)
N(2)–Cu(1)–N(1)	79.13(18)	N(2)–Cu(1)–Cl(2)	168.00(15)
N(1)–Cu(1)–Cl(2)	96.84(13)	N(2)–Cu(1)–O(2)	93.77(18)
N(1)–Cu(1)–O(2)	79.86(16)	Cl(2)–Cu(1)–O(2)	96.64(12)
N(2)–Cu(1)–Cl(1)	86.04(14)	N(1)–Cu(1)–Cl(1)	165.14(13)
Cl(2)–Cu(1)–Cl(1)	97.90(6)	O(2)–Cu(1)–Cl(1)	100.32(11)
N(3)–Cu(2)–N(6)	78.07(18)	N(3)–Cu(2)–Cl(3)	172.36(17)
N(6)–Cu(2)–Cl(3)	99.90(13)	N(3)–Cu(2)–O(3)	93.5(2)
N(6)–Cu(2)–O(3)	76.90(17)	Cl(3)–Cu(2)–O(3)	93.24(14)
N(3)–Cu(2)–Cl(1)	86.19(15)	N(6)–Cu(2)–Cl(1)	164.04(12)
Cl(3)–Cu(2)–Cl(1)	96.04(6)	O(3)–Cu(2)–Cl(1)	101.72(14)
Complex **2**			
Cu(1)–N(2)	1.938(8)	Cu(1)–N(1)	2.215(9)
Cu(1)–Br(4)	2.351(2)	Cu(1)–O(2)	2.371(8)
Cu(1)–O(1)	2.401(7)	Cu(1)–Br(3)	2.484(2)
Cu(2)–N(3)	1.924(8)	Cu(2)–N(6)	2.167(9)
Cu(2)–Br(2)	2.328(2)	Cu(2)–O(4)	2.400(8)
Cu(2)–Br(3)	2.453(2)	Cu(2)–O(3)	2.623(1)
Cu(1)···Cu(2)	3.899(2)		
N(2)–Cu(1)–N(1)	76.7(3)	N(2)–Cu(1)–Br(4)	178.4(2)
N(1)–Cu(1)–Br(4)	101.8(2)	N(1)–Cu(1)–Br(4)	101.8(2)
N(2)–Cu(1)–O(2)	92.2(4)	N(1)–Cu(1)–O(2)	75.5(3)
Br(4)–Cu(1)–O(2)	87.8(3)	N(2)–Cu(1)–O(1)	85.6(3)
N(1)–Cu(1)–O(1)	76.2(3)	Br(4)–Cu(1)–O(1)	93.55(19)
O(2)–Cu(1)–O(1)	151.3(3)	N(2)–Cu(1)–Br(3)	87.4(2)
N(1)–Cu(1)–Br(3)	164.0(2)	Br(4)–Cu(1)–Br(3)	94.15(6)
O(2)–Cu(1)–Br(3)	103.6(2)	O(1)–Cu(1)–Br(3)	104.85(18)
N(3)–Cu(2)–N(6)	79.5(3)	N(3)–Cu(2)–Br(2)	172.9(3)
O(4)–Cu(2)–Br(3)	100.7(2)	N(6)–Cu(2)–Br(2)	98.4(2)
N(3)–Cu(2)–O(4)	88.4(3)	N(6)–Cu(2)–O(4)	77.6(3)
Br(2)–Cu(2)–O(4)	97.75(18)	N(3)–Cu(2)–Br(3)	87.6(3)
N(6)–Cu(2)–Br(3)	166.9(2)	Br(2)–Cu(2)–Br(3)	94.64(6)

spectra of **1** and **2** binding to DNA were performed by increasing amounts of CT-DNA to the complexes in Tris-HCl buffer (pH 7.2).

Fluorescence Spectroscopic Studies: The relative bindings of complexes to CT-DNA were studied with an EB-bound CT-DNA solution in 5 mM Tris-HCl/50 mM NaCl buffer (pH 7.2). The fluorescence spectra were recorded at room temperature with excitation at 510 nm and emission at 602 nm. The experiments were carried out by titrating complexes into EB-DNA solution containing 5×10^{-5} M EB and 5×10^{-5} M CT-DNA.

CD Spectroscopic Studies: The CD spectra of CT-DNA in the presence or absence of a complex were collected in Tris-HCl buffer (pH 7.2) containing 50 mM NaCl at room temperature. All CD experiments were performed on a JASCO-J715 spectropolarimeter at room temperature from 350 to 230 nm.

Viscosity Experiments: Viscosity experiments were carried out using an Ubbelohde viscometer maintained at a constant temperature at (37.0 ± 0.1) °C in a thermostatic water bath. Flow time was measured with a digital stopwatch, each sample was measured three times and an average flow time was calculated. Data were presented as $(\eta/\eta_0)^{1/3}$ versus [complex]/[DNA], where η is the viscosity of CT-DNA in the presence of the complex and η_0 is the viscosity of CT-DNA alone in 5 mM Tris buffer medium. The viscosity values were calculated from the observed flow time of CT-DNA-containing solutions (t) and duly corrected for that of the buffer alone (t_0), $\eta = (t - t_0)$. According to Cohen and Eisenberg,[63] the relation between the relative solution viscosity (η/η_0) and contour length (L/L_0) is given by the following equation: $L/L_0 = (\eta/\eta_0)^{1/3}$, where L denotes the apparent molecular length in the absence of the metal complex.

Cyclic Voltammetry Studies: Cyclic voltammetry was performed on a BAS Epsilon Electrochemical Workstation with a three-electrode system consisting of a platinum glassy carbon as the working electrode, a platinum wire as the auxiliary electrode and a saturated calomel electrode (SCE) as the reference electrode. All the electrochemical measurements were carried out in a 10-mL electrolytic cell by using 10 mM Tris-HCl/50 mM NaCl buffer (pH 7.2) as the supporting electrolyte. Solutions were deoxygenated by purging with N_2 prior to measurements.

pBR322 DNN Cleavage Assay: The DNA cleavage experiments were done by agarose gel electrophoresis. The reaction was carried out following the literature method.[59] After electrophoresis, bands were visualized by UV light and photographed. Quantification of cleavage products was performed by UVI pro software, Version 10.03. Supercoiled plasmid DNA values were corrected by a factor of 1.3, based on the average literature estimate of lowered binding of ethidium.[64] Cleavage mechanistic investigation of pBR322 DNA was done using different reagents such as DMSO, EtOH, NaN_3, L-histidine, SOD, KI, SYBR Green, methyl green and EDTA added to pBR322 DNA prior to the addition of complexes.

Supporting Information (see also the footnote on the first page of this article): Agarose gel electrophoresis of DNA cleavage by the two copper(II) complexes in the presence of H_2O_2/ascorbate and ascorbate, absorption spectral and electrochemical data for the two complexes, respectively.

Acknowledgments

This work was supported by the National Natural Science Foundation of China (No. 20771063).

[1] M. E. Núñez, J. K. Barton, *Curr. Opin. Chem. Biol.* **2000**, *4*, 199–206.
[2] S. E. Wolkenberg, D. L. Boger, *Chem. Rev.* **2002**, *102*, 2477–2496.
[3] D. T. Thomas, A. G. Jason, *Curr. Opin. Chem. Biol.* **2005**, *9*, 127–134.
[4] J. D. West, L. J. Marnett, *Chem. Res. Toxicol.* **2006**, *19*, 173–194.
[5] S. Ferrer, R. Ballesteros, A. Sambartolome, M. Gonzalez, G. Alzuet, J. Borras, M. Liu, *J. Inorg. Biochem.* **2004**, *98*, 1436–1446.
[6] N. H. Williams, B. Takasaki, M. Wall, J. Chin, *J. Acc. Chem. Res.* **1999**, *32*, 485–493.
[7] B. Armitage, *Chem. Rev.* **1998**, *98*, 1171–1200.
[8] D. R. McMillin, K. M. McNett, *Chem. Rev.* **1998**, *98*, 1201–1220.
[9] W. K. Pogozelski, T. D. Tullius, *Chem. Rev.* **1998**, *98*, 1089–1108.
[10] C. J. Burrows, J. G. Muller, *Chem. Rev.* **1998**, *98*, 1109–1152.
[11] F. Mancin, P. Scrimin, P. Tecillab, U. Tonellato, *Chem. Commun.* **2005**, 2540–2548.
[12] J. A. Cowan, *Chem. Nucl.* **2001**, *5*, 634–642.
[13] M. G. Álvarez, G. Alzuet, J. Borrás, B. Macías, A. Castiñeiras, *Inorg. Chem.* **2003**, *42*, 2992–2998.
[14] M. Costas, M. P. Mehn, M. P. Jensen, L. Que Jr., *Chem. Rev.* **2004**, *104*, 939–986.

[15] G. Parkin, *Chem. Rev.* **2004**, *104*, 699–768.
[16] A. J. Wu, J. E. Penner-Hahn, V. L. Pecoraro, *Chem. Rev.* **2004**, *104*, 903–938.
[17] D. C. Crans, J. J. Smee, E. Gaidamauskas, L. Yang, *Chem. Rev.* **2004**, *104*, 849–902.
[18] L. M. Mirica, X. Ottenwaelder, T. D. P. Stack, *Chem. Rev.* **2004**, *104*, 1013–1046.
[19] W. J. Pogozelski, T. J. McNeese, T. D. Tullius, *J. Am. Chem. Soc.* **1995**, *117*, 6428–6433.
[20] Q. Jiang, N. Xiao, P. F. Shi, Y. G. Zhu, Z. J. Gou, *Coord. Chem. Rev.* **2007**, *251*, 1951–1972.
[21] R. M. Burger, *Chem. Rev.* **1998**, *98*, 1153–1170.
[22] B. K. Keppler, *New J. Chem.* **1990**, *14*, 389–403.
[23] P. G. Baraldi, M. G. Pavani, M. C. Nunez, P. Brigidi, B. Vitali, R. Gambari, R. Romagnoli, *Bioorg. Med. Chem.* **2002**, *10*, 449–456.
[24] F. Dallavalle, F. Gaccioli, R. Franchi-Gazzola, M. Lanfranchi, L. Marchiò, M. A. Pellinghelli, M. Tegoni, *J. Inorg. Biochem.* **2002**, *92*, 95–104.
[25] A. W. Addison, T. N. Rao, J. Reedijk, J. van Rijn, G. C. Verschoor, *J. Chem. Soc., Dalton Trans.* **1984**, *7*, 1349–1356.
[26] E. Spodine, A. M. Atria, J. Valenzuela, J. Jalocha, J. Manzur, A. M. García, M. T. Garland, O. Peña, J. Y. Saillard, *J. Chem. Soc., Dalton Trans.* **1999**, *17*, 3029–3034.
[27] M. Baldini, M. Belicchi-Ferrari, F. Bisceglie, P. P. Dall′Aglio, G. Pelosi, S. Pinelli, P. Tarasconi, *Inorg. Chem.* **2004**, *43*, 7170–7179.
[28] S. A. Tysoe, R. J. Morgan, A. D. Baker, T. C. Strekas, *J. Phys. Chem.* **1993**, *97*, 1707–1711.
[29] F. J. Meyer-Almes, D. Porschke, *Biochemistry* **1993**, *32*, 4246–4253.
[30] B. C. Baguley, M. LeBret, *Biochemistry* **1984**, *23*, 937–943.
[31] R. F. Pasternack, M. Cacca, B. Keogh, T. A. Stephenson, A. P. Williams, F. J. Gibbs, *J. Am. Chem. Soc.* **1991**, *113*, 6835–6840.
[32] J. R. Lakowicz, G. Webber, *Biochemistry* **1973**, *12*, 4161–4170.
[33] M. Cory, D. D. McKee, J. Kagan, D. W. Henry, J. A. Miller, *J. Am. Chem. Soc.* **1985**, *107*, 2528–2536.
[34] A. Rajendran, B. U. Nair, *Biochim. Biophys. Acta* **2006**, *1760*, 1794–1801.
[35] K. Karidi, A. Garoufis, N. Hadjiliadis, J. Reedijk, *Dalton Trans.* **2005**, 728–734.
[36] T. M. Kelly, A. B. Tossi, D. J. McConnell, T. C. Strekas, *Nucleic Acids Res.* **1985**, *13*, 6017–6034.
[37] X. L. Wang, H. Chao, H. Li, X. L. Hong, L. N. Ji, X. Y. Li, *J. Inorg. Biochem.* **2004**, *98*, 423–429.
[38] M. T. Carter, A. J. Bard, *J. Am. Chem. Soc.* **1987**, *109*, 7528–7531.
[39] J. P. Lancaster, *The Bioinorganic Chemistry of Nickel*, Wiley-VCH, New York, **1998**.
[40] B. Macías, M. V. Villa, F. Sanz, J. Borrás, M. González-Álvarez, G. Alzuet, *J. Inorg. Biochem.* **2005**, *99*, 1441–1448.
[41] A. Mazumder, C. L. Sutton, D. S. Sigman, *Inorg. Chem.* **1993**, *32*, 3516–3560.
[42] S. H. Chiou, N. Ohtsu, K. G. Bensch, in: *Biological and Inorganic Copper Chemistry* (Eds.: D. Karlin, J. Zubieta), Adenine Press, New York, **1985**, pp. 119–123.
[43] C. A. Detmer III, F. V. Pamatong, J. R. Bocarsly, *Inorg. Chem.* **1996**, *35*, 6292–6298.
[44] D. M. Kong, J. Wang, L. N. Zhu, Y. W. Jin, X. Z. Li, H. X. Shen, H. F. Mi, *J. Inorg. Biochem.* **2008**, *102*, 824–832.
[45] J. J. Li, R. Geyer, W. Tan, *Nucleic Acid Res.* **2000**, *28*, e52.
[46] M. E. Reichmann, S. A. Rice, C. A. Thomas, P. Doty, *J. Am. Chem. Soc.* **1954**, *76*, 3047–3053.
[47] D. Gibellini, F. Vitone, P. Schiavone, C. Ponti, M. L. Placa, M. C. Re, *J. Clin. Virol.* **2004**, *29*, 282–289.
[48] F. B. El Amrani, L. Perelló, J. A. Real, M. González-Alvarez, G. Alzuet, J. Borrás, S. García-Granda, J. Montejo-Bernardo, *J. Inorg. Biochem.* **2006**, *100*, 1208–1218.
[49] T. B. Thederahn, M. D. Kuwabara, T. A. Larsen, D. S. Sigman, *J. Am. Chem. Soc.* **1989**, *111*, 4941–4946.
[50] D. S. Sigman, *Acc. Chem. Res.* **1986**, *19*, 180–186.
[51] H. Sies, *Eur. J. Biochem.* **1993**, *215*, 213–219.
[52] M. Masarwa, H. Cohen, D. Meyerstein, D. L. Hickman, A. Bakac, J. H. Espenson, *J. Am. Chem. Soc.* **1988**, *110*, 4293–4297.
[53] S. Oikawa, O. Kawanishi, *Biochemistry* **1996**, *35*, 4584–4590.
[54] K. Yamamoto, S. Kawanishi, *J. Biol. Chem.* **1989**, *264*, 15435–15440.
[55] G. Mezei, R. G. Raptis, *Inorg. Chim. Acta* **2004**, *357*, 3279–3288.
[56] R. Boča, L. Dlháň, G. Mezei, T. Ortiz-Pérez, R. G. Raptis, J. Telser, *Inorg. Chem.* **2003**, *42*, 5801–5803.
[57] J. L. Chou, J. P. Chyn, F. L. Urbach, D. F. Gervasio, *Polyhedron* **2000**, *19*, 2215–2223.
[58] G. Ambrosi, P. Dapporto, M. Formica, V. Fusi, L. Giorgi, A. Guerri, M. Micheloni, P. Paoli, R. Pontellini, P. Rossi, *Inorg. Chem.* **2006**, *45*, 304–314.
[59] G. M. Sheldrick, *SHELXS-97, Program for the Solution of Crystal Structure*, University of Göttingen, Germany, **1997**.
[60] G. M. Sheldrick, *SHELXL-97, Program for the Refinement of Crystal Structure*, University of Göttingen, Germany, **1997**.
[61] J. Marmur, *J. Mol. Biol.* **1961**, *3*, 208–218.
[62] Y. Gultneh, A. R. Khan, D. Blaise, S. Chaudhry, B. Ahvazi, B. B. Marvey, R. J. Butcher, *J. Inorg. Biochem.* **1999**, *75*, 7–18.
[63] G. Cohen, H. Eisenberg, *Biopolymers* **1969**, *8*, 45–55.
[64] F. V. Pamatong, C. A. Detmer, J. R. Bocarsly, *J. Am. Chem. Soc.* **1996**, *118*, 5339–5345.

Received: August 4, 2009
Published Online: October 21, 2009

